Inhibition of protein disulfide isomerase induces differentiation of acute myeloid leukemia cells

Justyna Chlebowska-Tuz,[1,2,3] Olga Sokolowska,[1,2,4] Pawel Gaj,[1,5] Michal Lazniewski,[6,7] Malgorzata Firczuk,[1] Karolina Borowiec,[1] Hanna Sas-Nowosielska,[8] Malgorzata Bajor,[1] Agata Malinowska,[9] Angelika Muchowicz,[1] Kavita Ramji,[1] Piotr Stawinski,[10] Mateusz Sobczak,[2] Zofia Pilch,[1] Anna Rodziewicz-Lurzynska,[11] Malgorzata Zajac,[12] Krzysztof Giannopoulos,[12] Przemyslaw Juszczynski,[13] Grzegorz W. Basak,[14] Dariusz Plewczynski,[6,15] Rafal Ploski,[10] Jakub Golab[1,16] and Dominika Nowis[1,2,17]

[1]Department of Immunology, Medical University of Warsaw; [2]Laboratory of Experimental Medicine, Center of New Technologies, University of Warsaw; [3]Institute of Genetics and Biotechnology, Faculty of Biology, University of Warsaw; [4]Postgraduate School of Molecular Medicine, Medical University of Warsaw; [5]Laboratory of Human Cancer Genetics, Center of New Technologies, University of Warsaw; [6]Laboratory of Functional and Structural Genomics, Center of New Technologies, University of Warsaw; [7]Department of Physical Chemistry, Faculty of Pharmacy, Medical University of Warsaw; [8]Laboratory of Imaging Tissue Structure and Function, Nencki Institute of Experimental Biology, Polish Academy of Sciences, Warsaw; [9]Laboratory of Mass Spectrometry, Institute of Biochemistry and Biophysics, Polish Academy of Sciences, Warsaw; [10]Department of Medical Genetics, Center of Biostructure Research, Medical University of Warsaw; [11]Department of Laboratory Diagnostics, Faculty of Health Sciences, Medical University of Warsaw; [12]Department of Experimental Hematooncology, Medical University of Lublin; [13]Department of Experimental Hematology, Institute of Hematology and Transfusion Medicine, Warsaw; [14]Department of Hematology, Oncology and Internal Diseases, Medical University of Warsaw; [15]Faculty of Mathematics and Information Science, Warsaw University of Technology, Warsaw; [16]Center for Preclinical Research and Technology, Medical University of Warsaw and [17]Genomic Medicine, Medical University of Warsaw, Poland

 doi:10.3324/haematol.2018.190231

Received: February 3, 2018.

Accepted: July 10, 2018.

Pre-published: July 12, 2018.

Correspondence: d.nowis@cent.uw.edu.pl or jakub.golab@wum.edu.pl

Inhibition of protein disulfide isomerase induces differentiation of AML cells

Supplementary data

Supplementary Materials and Methods

SK053 and its analogues. Chemical structures of SK053 and its analogs (Supplementary Fig. S6A-C) were created using Marvin Sketch software ver. 15.9.28, Chem Axon Ltd, Cambridge, MA, USA. Details of chemical synthesis of SK053 are described elsewhere.[1]

AML cell lines. KG1 (ATCC-CCL-246), HL-60 (ATCC-CCL-240), HeLa (ATCC-CCL-2) and HS-5 (ATCC-CRL-11882) were purchased from American Type Culture Collection (ATCC, LGC Standards, Teddington, UK). NB4 (ACC 207) cell line was purchased from German Collection of Microorganisms and Cell Cultures (DSMZ, Braunschweig, Germany). MOLM14 cell line was kindly provided by Prof. Przemyslaw Juszczynski (Department of Experimental Hematology, Institute of Hematology and Transfusion Medicine, Warsaw, Poland).

AML cell lines culture conditions. NB4, MOLM14, HS-5 and HL-60 cells were cultured in RPMI 1640 (Sigma-Aldrich) supplemented with 10% heat-inactivated fetal bovine serum (Hyclone), 100 µg/ml streptomycin, 100 U/ml penicillin (Sigma-Aldrich). KG1 cells were cultured in IMDM (Gibco) supplemented with 20% heat-inactivated fetal bovine serum (Hyclone) and antibiotics as stated above. HeLa cells were cultured in DMEM (Gibco) supplemented with 10% heat-inactivated fetal bovine serum (Hyclone) and antibiotics as stated above. All cells were cultured at 37°C in a fully humidified atmosphere of 5% CO2. In all experiments, cells were incubated with SK053, all-trans retinoic acid (ATRA; Sigma-Aldrich) or phorbol esters (PMA; Sigma-Aldrich) as positive control for differentiation and 0.1% dimethyl sulfoxide (DMSO; Sigma-Aldrich) as solvent control. Medium with drugs was replaced every third day of incubation time. Compounds stocked dissolved in DMSO were stored at –20°C until used.

Cell viability and growth assessment. For trypan blue exclusion assay cells were plated in triplicates at 2×10^5 cells per well in 12-well culture plates in 1 ml of culture medium with indicated SK053 concentrations. Cell numbers and viability were estimated with trypan blue (Sigma-Aldrich) exclusion assay, by counting cells from each well in duplicates in Bürker chamber (Heinz Herenz Medizinalbedarf, Hamburg, Germany). Percentage of dead cells was also evaluated in flow cytometry with propidium iodide (PI; 2 µg/ml, Sigma-Aldrich) using LSR II Fortessa cytometer (BD Biosciences, San Jose, CA, USA) and BD FACSDiva software version 8 (BD Biosciences). For trypan blue exclusion assay (Fig. 4F, Supplementary Fig. S6C,D) cells were plated in duplicates at 2×10^5 cells per well in 12-well culture plates in 1 ml of culture medium with indicated SK053 concentrations. Cell numbers and viability were estimated with trypan blue (Bio-Rad) exclusion assay, by counting cells from each well in duplicates in TC20 Automated Cell Counter (Bio-Rad).

AML differentiation assays. For differentiation experiments, cells were seeded at a density of 2×10^5 cells/ml in 6-well plate and treated with indicated concentrations of SK053. In some experiments 1 µM ATRA, 5 µM ATRA or 50 ng/ml PMA served as positive differentiation controls for APL (HL-60, NB4), MOLM14 and KG1 cell lines, respectively. To examine cellular morphology, cells were cytospun using Cytospin4 centrifuge (Thermo Fisher Scientific) at 100×g for 10 min at RT, stained with May Grünwald-Giemsa (MGG; Merck KGaA, Darmstadt, Germany) and observed using Eclipse 80i (Nikon) microscope equipped with QICAM Fast 1394 camera (QImaging, Surrey, BC, Canada and Image Pro Plus

software version 7.0 (Media Cybernetics, Rockville, MD, USA). Myeloid differentiation was assessed by surface expression of CD11b. Briefly, 3×10^5 cells were collected, washed with PBS and incubated for 30 min at RT with anti-human anti-CD11b-Alexa Fluor488 antibodies, cat. no. 11-0118-42 (eBioscience, Thermo Fisher Scientific) diluted in 2% bovine serum albumin (BSA; Sigma-Aldrich) followed by PBS wash and viability staining with 7AAD (eBioscience) according to manufacturer's protocol. Fluorescence intensity was evaluated using FACSCanto II flow cytometer (BD Biosciences) and analyzed with FlowJo software version 10.2 (FlowJo LLC). Conventional semi-quantitative microscopic nitroblue tetrazolium (NBT; Sigma-Aldrich) assay was used to determine the production of superoxide anion upon stimulation with PMA in differentiated AML cells. To this end, 1×10^6 of cells were collected, washed with PBS and suspended in 100 µl RPMI 1640 and mixed with an equal volume of 2 mg/ml NBT dissolved in PBS containing 2 µg/ml PMA and incubated at 37°C for 2 h. Microscopic observation revealed cells containing blue NBT formazan deposits in MGG stained slides. Moreover, modified quantitative NBT assay was established and implemented by dissolving the blue formazan particles from equal cell numbers in 100 µL of 2M sodium hydroxide, followed by measurement of absorbance at 620 nm using ASYS UVM 340 microplate reader (Biochrom, Cambridge, UK).

HS5 and HL-60 co-culture. Cytostatic/cytotoxic effects of SK053 on HL-60 cells in coculture with stroma cell line HS5 was performed using a transwell system (Falcon; cat. No. 734-0038, Thermo Fisher Scientific). HS5 cells were seeded at a density 5×10^4 /well on 24-well plate in 0.5 ml medium into the lower compartment of transwell. Next, 3×10^4 of HL-60 cells were seeded into the upper compartment. Medium with SK053 was changed every day. Upon 72 h incubation with SK053, the cytostatic/cytotoxic effects were assessed using propidium iodide staining (final concentration 2.5 µg/ml; Sigma-Aldrich). Red fluorescence was analyzed in LSR Fortessa flow cytometer (BD Biosciences) and FlowJo software version 10.2 (FlowJo LLC, Ashland, OR, USA) and BD FACSDiva software version 8 (BD Biosciences).

LICs assessment. Surface expression of CD34, CD38 and CD123 markers was used to evaluate the percentage of leukemia initiating cells (LICs) in KG1 cell line incubated for the indicated times with SK053. For the analysis 5×10^5 cells were collected, washed with PBS and incubated for 30 min at RT with anti-human mAbs - anti-CD34-APC, cat. no. 555824; anti-CD38-V450, cat. no. 646851, anti-CD123-PerCP-Cy5.5, cat. no. 558714 (all obtained from BD Biosciences, San Jose, CA, USA) diluted according to manufacturer's protocol in 2% BSA. Cells were washed with PBS and flow cytometry analysis was performed on the LSR II Fortessa cytometer (BD Biosciences) with BD FACSDiva software version 8 (BD Biosciences) or FlowJo software version 10.2 (FlowJo LLC).

Colony formation assay. To determine the clonogenic potential, KG1 cells were pre-treated for 72h with SK053, washed with PBS and then 5×10^3 cells were plated in triplicates in cytokine-enriched methylcellulose (MethoCult™Optimum Without EPO, Cat. No H4035, StemCell Technologies, Inc.) on Smart Dishes (Cat. No 27371 StemCell Technologies, Inc). Colonies containing more than 20 cells were counted after 14 days of culture. Images of colonies were acquired using Olympus CKX52 microscope and analyzed with ImageJ software (https://imagej.nih.gov/).

Incubation of recombinant proteins with SK053. For mass spectrometry and binding assays huPDI protein was reduced by 15-min incubation with 10 mM DTT at 37°C followed by a dialysis to 10 mM Tris pH7.5 and 30-min incubation with a 10× molar excess of SK053 at 37°C. To oxidize –SH groups of PDI for binding assays, the protein was left in the fridge for 24 or 48 h. Next, 10 µg of reduced or oxidized huPDI was incubated for 30 min at 37°C with a 10× molar excess of SK-BIO. 200 ng of each protein was separated with SDS-PAGE followed by Western blotting using anti-biotin monoclonal antibody (Supplementary Tab. S9). Gels stained with Coomasie blue (Bio-Rad, Hercules, CA, USA) served as loading controls.

PDIA1-d4 reduced with 5mM DTT was incubated with SK053 in 1:10 molar ratio for 30 min at 37°C in 10 mM Tris buffer, pH 7.5. The binding of SK053 to PDIA1-d4 was assessed by mass spectrometry using LTQ Orbitrap Velos mass spectrometer (ThermoElectron).

Gene silencing using ready to use lentivirus-expressed shRNAs. Ready to use MISSION pLKO.1-puro shRNA lentivirus particles targeting TXN [TXN(a)], PDI [PDI(a), PDI(b)] as well as non-targeting shRNA scramble control (NTC) (Supplementary Tab. S10) were purchased from Sigma-Aldrich. Transduction was performed according to the manufacturer's instructions. At 72 h post transduction successfully infected HL-60 cells were selected with 2 µg/ml puromycin (Sigma-Aldrich), knock-down was validated by Western blotting 5 days post transduction. PDI(b) hairpin did not silence P4HB expression.

Gene silencing using custom packaged lentivirus-expressed shRNAs. Lentiviruses for shRNA were produced by co-transfecting (calcium chloride) HEK293T cells with MISSION pLKO.1-puro shRNA plasmids targeting TXN [TXN(b), TXN(c), TXN(d)], PDI [PDI(c), PDI(d), PDI (e)], CEBPA [CEBPA(a), CEBPA(b), CEBPA (c)] as well as non-targeting shRNA scramble control (NTC) (Supplementary Tab. S10) (Sigma-Aldrich) together with packaging plasmids pMD2.G and psPAX2 (pMD2.G and psPAX2 plasmids were generous gifts from prof. Didier Trono (Ecole polytechnique federale de Lausanne, Switzerland).Transduction was performed according to the manufacturer's instructions. At 72 h post transduction successfully infected cells were selected with 2 µg/ml puromycin (Sigma-Aldrich), knock-down was validated by Western blotting 7 days post transduction. TXN(d), CEBPA(b) and PDI(c) hairpins did not silence expression of the corresponding genes. PDI(e) hairpin showed off target effects (silenced ERO1α expression).

RNA extraction and quantitative Real-Time PCR

RNA concentration was measured with NanoDrop spectrophotometer (Thermo Fisher Scientific). A total of 0.5 µg RNA was used for cDNA synthesis primed with oligo(dT) using Native AMV Reverse Transcriptase (EurX, Gdansk, Poland) in a final volume of 10 µl. For each qPCR run, the samples were measured in duplicates to estimate their reproducibility. Primers sequences and probes numbers are shown in Supplementary Tab. S8. Samples in which the cDNA was omitted were used as negative controls. The results were analyzed after 40 cycles of amplification using LightCycler 480 Software 1.5 and normalized for the content of the housekeeping genes (β2-microglobulin and ribosomal protein L29). The fold change for each gene was calculated using a user-non-influent, second derivative method. The specificity of the reactions was confirmed by analysis of the PCR product in 2% agarose gel.

Immunoprecipitation. HL-60 cells (5×10^6) were incubated for 4 h in culture media without FBS containing 100 µM SK-BIO or SK-IN. Next, the cells were lysed in 0.1% (v/v) NP-40 in PBS supplemented with Complete protease inhibitors cocktail (Roche). Equal amounts of proteins were incubated with 5 µg of anti-tioredoxin (TXN) (Abcam, Cambridge, UK; clone 3A1) antibody per 500 ml of lysate, 5 µg of anti-PDI (Abcam; clone RL90) antibody per 500 ml of lysate or without antibodies for 2 h at room temperature (RT) with gentle agitation. Next, protein G-coated beads (Pierce, Thermo Fisher Scientific) were added to the lysates for the subsequent 16 h incubation at 4°C with gentle agitation. After extensive washes with lysis buffer, beads-bound proteins were eluted by boiling in SDS sample buffer. Then, 20 µL of samples were electrophoresed and probed with anti-TXN, anti-PDI, and anti-biotin antibodies using working concentrations as described in Supplementary Tab. S9.

PDI enzymatic assay. PDI enzymatic activity was assessed in a turbidimetric assay measuring the thiol isomerase-catalyzed reduction of insulin in the presence of DTT. The absorption of aggregated reduced insulin chains was measured at 650 nm using Asys UV340M plate reader (Biochrom). The enzymatic activity assay mixture was prepared in the final volume of 150 µl. Briefly, 1.7 µM recombinant PDI protein was preincubated for 1h at

37°C with indicated SK053 concentrations in the presence of 2 mM EDTA in 100 mM potassium phosphate buffer, pH 7.4. Next, 135 µL of 270 µM DTT (Thermo Fisher Scientific) and 545 µM of bovine insulin (Sigma-Aldrich) mixture dissolved in reaction buffer was added. The plate was incubated at 25°C and absorbance was read every 5 min for subsequent 60 min. IC50 was determined using SigmaPlot software (Systat Software Inc., San Jose, CA, USA).

Fluorescence lifetime measurements by time-correlated single-photon counting (TCSPC)

The day before transfection HeLa cells were plated 2.5×105 cells per well on 35 mm glass bottom dishes (Cell E&G, San Diego, CA, USA) covered with poly-L-lysine (Sigma-Aldrich) and then cells were transfected with 2 µg of roGFPiE containing plasmid [2] (kindly provided by Professor David Ron from University of Cambridge Metabolic Research Laboratories and NIHR Cambridge Biomedical Research Centre, Cambridge, UK) using 5 µL Lipofectamine 3000 (Invitrogen, Thermo Fisher Scientific), according to the manufacturer's protocol. Next day, cells were incubated with DMSO (solvent control) for 8h, 25 µM SK053 for 8h or 100 µM DTT for 30 min. Fluorescence lifetime imaging (FLIM) data were collected using SP8 confocal microscope equipped with TCSPC module (PicoHarp300, PicoQuant, Berlin, Germany). Moreover the system was equipped with an incubation chamber suitable to maintain the live cells and optics at 37°C, 63× water immersion NA 1.2 objective lens and with confocal pinhole set to 2 Airy units. To excite GFP fluorescence white light laser with wavelength set to 488 nm and 40 kHz repetition rate was used. GFP fluorescence was detected in 500-550 nm band with APD detector. FLIM data were collected in TCSPC mode using PicoHarp300 (PicoQuant). To avoid photo toxicity and minimize perturbations due to cells motility, FLIM images were collected 64×64 pixel format, with pixel size set to 14 µm. FLIM data were collected until 5000 counts in the brightest pixel of an image were acquired. Data analysis and fitting were performed using FLIMfit software (Imperial College London, UK).

Western blot. HL-60 cells were washed twice with ice-cold PBS, lysed in RIPA buffer (50 mmol/L Tris base, 150 mmol/L NaCl, 1% NP-40, 0.25% sodium deoxycholate, and 1 mmol/L EDTA) or cytoplasmic/nuclear fractions of proteins were extracted using NE-PER Kit (Pierce). Lysis buffers were supplemented with Complete protease inhibitor cocktail (Roche). The lysates were then cleared by centrifugation at 15,000×g for 10 min. Protein concentration in supernatants was evaluated with Bio-Rad Protein Assay (Bio-Rad). Next, samples were boiled for 5 min in 5× Laemmli Sample Buffer. Equal amounts of lysates were subjected to SDS-PAGE, transferred onto a nitrocellulose membrane (Schleicher and Schuell, Sigma-Aldrich) and then blocked with Tris-buffered saline (pH 7.4) and 0.05% Tween 20 supplemented with 5% BSA. Next, membranes were probed with primary (listed in Supplementary Tab. S9) and corresponding HRP-coupled secondary antibodies (Jackson ImmunoResearch, West Grove, PA, USA) before visualization using self-made chemiluminescence reagent (100 mM Tris pH 8.0, 1.25 mM luminol, 0.2 mM coumaric acid, 0.006% hydrogen peroxide) with Stella 8300 bioimager (Raytest, Angleur, Belgium).

RNA-seq libraries preparation. A total of 1 µg RNA was treated with Turbo-DNase (Life Technologies) according to the manufacturer's instructions. Then, rRNA was removed from samples using a Ribo-Zero Kit (Epicentre) according to the manufacturer's protocol, and samples were spiked-in with external RNA (ERCC RNA Spike-In Mix; Life Technologies). RNA libraries were prepared using KAPA Stranded RNA-Seq Library Preparation Kit (Kapa Biosystems) according to the manufacturer's instructions. Quality of libraries was determined by chip electrophoresis performed using the Agilent 2100 Bioanalyzer (Agilent Technologies, Inc.).

RNA-seq data acquisition and analysis. Ribo-depleted total RNA isolated from HL-60 cell line incubated with SK053 in duplicates were used to prepare strand-specific libraries (dUTP

RNA). These libraries were subsequently sequenced using an Illumina HiSeq sequencing platform to the average number of 21.9 million reads per sample in 100-nt pair-end mode. The quality control of obtained sequences was performed using FastQC software. Reads were than mapped to the reference human genome (hg19) using STAR short-read aligner yielding an average of 76.4% uniquely mapped reads. Read processing, filtering and counting were performed using HTseq software. Differential expression analyses were performed using the EdgeR following gene filtration and raw read count normalization against differences in library sizes using TMM algorithm. The Gene Ontology (GO) (BP: Biological Process or MF: Molecular Function) enrichment analysis was carried out in Cytoscape (BiNGO) and topGO using the lists of differentially expressed genes (FDR<0.01) between cells incubated with SK053 and the control cells (DMSO). The background set of genes used in the GO analysis consisted of the filtered set of genes previously used in the RNAseq DGE analysis. The results were adjusted for multiple hypothesis testing using Benjamini-Hochberg FDR method.

Expression of human PDI. cDNA encoding human PDI was cloned and expressed in a prokaryotic protein expression system followed by nickel affinity chromatography and subsequent gel filtration as described.[1]

Cloning, expression, purification of d4 domain (4th thioredoxin-like domain) of huPDIA1. The d4 domain of human PDIA1 protein, corresponding to the sequence encoding amino acids 368-475, was amplified by PCR using the following primers: FPDIA1d4: 5' GGCGAATTCCCTGTCAAGGTGCTTGTTGG and RPDIA1d4: 5' GGCCTCGAGTTATTGGCCACCGCTCTCTAGG. cDNA from human prostate cancer cell line DU-145 (ATCC No HTB-81) was used as a template. The PCR product was cloned into EcoRI and XhoI recognition sites of pET15-mod plasmid, a derivative of Novagen pET15b(+) vector, containing 6 N-terminal histidine codons (a generous gift from Prof. Mattias Bochtler from the International Institute of Molecular and Cell Biology, Warsaw, Poland). The sequence of the insert was confirmed by Sanger sequencing. For protein expression, the plasmid pET15-mod-PDIA1-d4 was transformed to *E. coli* Rosetta strain. Cells were grown at 37°C until reached OD_{600} = 0.6-0.7, at which point 1 mM isopropyl β-D-1-thiogalactopyranoside (IPTG) was added and the cultures were shifted to 30°C for additional 20 h. Recombinant protein was purified by nickel affinity and gel filtration chromatography as described.[3]

Pulldown of SK-BIO binding proteins and mass spectrometry. HL-60 cells (30×10^6) were incubated for 4h in culture media without FBS containing 100 μM of biotinylated enzymatically active analogs of SK053 (referred to as SK-BIO, Supplementary Fig. S1B) or an inactive analog lacking electrophile group attacking the nucleophilic cysteine residues (referred to as SK-IN, Fig. S1C). After cell lysis and extensive washes, beads-bound proteins were eluted with 5 mM biotin (Sigma-Aldrich), 5 mM biotin and 5 mM urea (Avantor Performance Materials, Gliwice, Poland) or by boiling in SDS sample buffer. Band detected in 12% polyacrylamide silver stained gel in SK-BIO sample was excised and analyzed by mass spectrometry using LTQ Orbitrap Velos mass spectrometer (ThermoElectron, San Jose, CA, USA). The obtained reads were compared with NCBI, UniProt database and analyzed using Mascot software.

Mass spectrometry of huPDI incubated with SK053. Following incubation with 10 x molar excess of SK053, 30 μg of recombinant huPDI was digested overnight with 10 ng/μL trypsin (Promega, Madison, WI, USA), then reduced with 100 mM DTT for 30 min at 56°C, and alkylated with 50 mM iodoacetamide in the dark for 45 min at 24°C. The resulting peptide mixtures were applied to an RP-18 precolumn (Waters, Milford, MA, USA) using water that contained 0.1% formic acid as a mobile phase and then transferred to the RP-18 column (75 μM internal diameter; Waters) of the nanoACQUITY UPLC system (Waters) using an ACN gradient (0–30% ACN in 45 min) in the presence of 0.1% formic acid at a flow rate of 250

nL/min. The column outlet was coupled directly to the ion source of an LTQ Orbitrap Velos mass spectrometer (ThermoElectron, San Jose, CA, USA) working in the regime of data-dependent MS to MS/MS switch. Two blank runs that ensured the absence of cross-contamination from previous samples preceded each analysis. The obtained mass spectra were preprocessed with MascotDistiller software (v. 2.2.1, Matrix Science, Manchester, UK). The search parameters were set to the following: enzyme (semiTrypsin), variable modifications (cysteine carbamidomethylation, methionine oxidation, and SK053 modification) and the mass shift (282.157957 Da) for cysteine modification was calculated.

Molecular Dynamics simulation. To perform ensemble docking, a set of conformations of the reduced form of human PDI (pdb|4ekz) was generated using molecular dynamics simulation. The MD simulation was performed with the OpenMM program[4] using the AMBER99sb force field and TIP3P water molecules (explicit solvent) with periodic boundary conditions. The thickness of the water box was 0.8 nm. Non-bond interactions were truncated at 1 nm. The simulation consisted of 3 stages: a 40 ps cooling to 0°K, a 100 ps warming to 300°K and a 20-ns production run. The unrestrained production run was carried out at a constant temperature (300°K) using the Langevin thermostat with a collision frequency of 1 ps-1 and at a constant pressure (1 atm) using a MonteCarlo barostat. The trajectories during production run were saved every 10 ps generating a total 2,000 conformations.

Conformation selection. Out of 2000 conformations obtained with MD simulation 90 were chosen for further analysis with ensemble molecular docking. Three criteria were chosen, each independently selecting 30 conformations. First, the best 30 conformations with the lowest total energy among those obtained in the production run were selected. Second, an RMSD matrix was calculated for all 2000 conformations and was subsequently used for clustering using an agglomerative clustering algorithm with UPGMA criterion. The clustering produced 30 clusters out of which a single medoid conformation was chosen. The final 30 conformations where selected based on their ability to represent the variability of distance observed between the sulfur atom of Cys397 and the sulfur atom of Cys400.

Covalent docking of SK053 to human PDI. In the next step, covalent docking of truncated SK053 (lacking the leaving group, Fig. S1d), to the previously selected 90 conformations was performed using the GOLD program.[5] The covalent docking site was defined as a sphere of 12 Å radius centered at the Cys400 sulfur atom. Covalent docking simulations to Cys400 and Cys397 were carried out independently. Prior to docking, a pair of atoms that form a covalent bond was specified and all the water molecules present after MD simulation were removed. Otherwise, the docking studies were performed using the program's default settings. For each GA run, a maximum of 100,000 operations was performed on a set of five groups with a population of 100 individuals. The annealing parameters were used as default: cutoff values of 3.0 Å for hydrogen bonds and 4.0 Å for van der Waals interactions. Early termination of the calculations was allowed if the RMSD of the three highest scored conformations were within 1.5 Å. The docking score between PDI and SK053 was calculated using the GoldScore energy based scoring function, which takes into account intra- and intermolecular hydrogen bonding interaction energy, van der Waals energy and ligand torsion energy.

Supplementary references

1. Muchowicz A, Firczuk M, Chlebowska J, Nowis D, Stachura J, Barankiewicz J, et al. Adenanthin targets proteins involved in the regulation of disulphide bonds. Biochem Pharmacol. 2014;89(2):210-6.

2. Avezov E, Cross BC, Kaminski Schierle GS, Winters M, Harding HP, Melo EP, et al. Lifetime imaging of a fluorescent protein sensor reveals surprising stability of ER thiol redox. J Cell Biol. 2013;201(2):337-49.

3. Klossowski S, Muchowicz A, Firczuk M, Swiech M, Redzej A, Golab J, et al. Studies toward novel peptidomimetic inhibitors of thioredoxin-thioredoxin reductase system. J Med Chem. 2012;55(1):55-67.

4. Eastman P, Friedrichs MS, Chodera JD, Radmer RJ, Bruns CM, Ku JP, et al. OpenMM 4: A Reusable, Extensible, Hardware Independent Library for High Performance Molecular Simulation. J Chem Theory Comput. 2013;9(1):461-9.

5. Jones G, Willett P, Glen RC, Leach AR, Taylor R. Development and validation of a genetic algorithm for flexible docking. J Mol Biol. 1997;267(3):727-48.

Descriptions to supplementary tables

Supplementary Table S1. Genes differentially expressed between HL-60 cells treated for 48 h with 10 μM SK053 and control cells (DMSO).

Supplementary Table S2. Results of Gene Ontology (Biological Process) analysis carried out in *Cytoscape {BiNGO}c* using the list of genes differentially expressed (FDR < 0.01) between HL-60 cells treated for 48 h with 10 μM SK053 and the control cells (DMSO).

Supplementary Table S3. Results of Gene Ontology (Molecular Function) analysis carried out in *Cytoscape {BiNGO}* using the list of genes differentially expressed (FDR < 0.01) between HL-60 cells treated for 48 h with 10 μM SK053 and the control cells (DMSO).

Supplementary Table S4. Genes differentially expressed between HL-60 cells treated for 120 h with 10 μM SK053 and control cells (DMSO).

Supplementary Table S5. Results of Gene Ontology (Biological Process) analysis carried out in *Cytoscape {BiNGO}* using the list of genes differentially expressed (FDR < 0.01) between HL-60 cells treated for 120 h with 10 μM SK053 and the control cells (DMSO).

Supplementary Table S6. Results of Gene Ontology (Molecular Function) analysis carried out in *Cytoscape {BiNGO}* using the list of genes differentially expressed (FDR < 0.01) between HL-60 cells treated for 120 h with SK053 and the control cells (DMSO).

Supplementary Table S7 - Top proteins pulled down using biotinylated SK053 from HL-60 AML cells identified in mass spectrometry

gi|39794653	Keratin 1 [Homo sapiens]
gi|375314779	keratin 1 [Homo sapiens]
gi|435476	cytokeratin 9 [Homo sapiens]
gi|119617047	keratin 2A (epidermal ichthyosis bullosa of Siemens) [Homo sapiens]
gi|119581084	keratin 10 (epidermolytic hyperkeratosis; keratosis palmaris et plantaris), isoform CRA_a [Homo sapiens]
gi|122920512	Chain A, Human Serum Albumin Complexed With Myristate And Aspirin
gi|119587944	heat shock 70kDa protein 8, isoform CRA_a [Homo sapiens]
gi|386785	heat shock protein [Homo sapiens]
gi|194388088	unnamed protein product [Homo sapiens]
gi|292059	MTHSP75 [Homo sapiens]
gi|158255142	unnamed protein product [Homo sapiens]
gi|47940601	Keratin 5 [Homo sapiens]
gi|63100331	Keratin 14 [Homo sapiens]
gi|410171504	PREDICTED: hornerin [Homo sapiens]
gi|1143492	BiP [Homo sapiens]
gi|31074631	keratin 1b [Homo sapiens]
gi|119617032	keratin 6B, isoform CRA_a [Homo sapiens]
gi|119600472	protein disulfide isomerase family A, member 4, isoform CRA_a [Homo sapiens]
gi|38013966	TKT protein [Homo sapiens]
gi|687237	tumor necrosis factor type 1 receptor associated protein, partial [Homo sapiens]
gi|148271059	dermcidin [Homo sapiens]
gi|119581157	keratin 17, isoform CRA_d [Homo sapiens]
gi|3983129	desmoglein 1 [Homo sapiens]
gi|31873640	hypothetical protein [Homo sapiens]
gi|74096732	filaggrin 2 [Homo sapiens]
gi|119617046	keratin 6 irs3 [Homo sapiens]
gi|184761	immunoglobulin alpha-2 heavy chain [Homo sapiens]
gi|21755908	unnamed protein product [Homo sapiens]

Supplementary Table S8 - Primers and probes used for quantitative PCR

Name	Accession No.	Forward primer (5'-3'):	Reversed primer (5'-3'):	UPL#
β_2-microglobulin	NM_004048.2	TAGGAGGGCTGGCAACTTAG	CCAAGATGTTGATGTTGGATAAGA	42
ribosomal protein L29	NM_000992.2	CAGCTCAGGCTCCCAAAC	GCACCAGTCCTTCTGTCCTC	53
CEBPA	NM_004364.3	GGAGCTGAGATCCCGACA	TTCTAAGGACAGGCGTGGAG	28
CEBPB	NM_005194.2	GCGACGAGTACAAGATCC	AACAAGTTCCGCAGGGTG	74
MPO	NM_000250.1	TTCGTCACTGGCGTCAACT	ATTGGGCGGGATCTTGAG	38
ELANE	NM_001972.2	TTCCTCGCCTGTGTCCTG	CTGCAGGGACACCATGAA	3
GCSFR	NM_000760.3	AGCGCGAGCAATAGCAAC	TGAAAGGGCCTGATGTTCTC	23
GMCSFR	NM_001161529.1	AGTCTCCGAGAGAAGAAAAGCA	CGGATTTTCCTGCTGTAAACC	12
HK3	NM_002115.2	CCTCCCACTGGGTTTTACCT	GAAACCCTTGGTCCAGTTCA	37
SOX4	NM_003107.2	AGCCGGAGGAGGAGATGT	TTCTCGGGTCATTTCCTAGC	20

Supplementary Table S9 - Antibodies used for Western blot analyses

Antibody target	**Source and cat. no.**	**Manufacturer**	**Working concentration**
PDI	(C81H6) rabbit mAb #3501	Cell Signaling	1:1000
actin-HRP conjugated	mAb A3854	Sigma-Aldrich	1:50,000
α-Tubulin	(DM1A) mouse mAb CP06	Calbiochem	1:1000
C/EBPα	rabbit polyclonal ab15048	Abcam	1:1000
HDAC2	rabbit polyclonal#2540	Cell Signaling	1:1000
Thioredoxin 1	(C63C6) rabbit mAb #2429	Cell Signaling	1:1000
Biotin-HRP conjugated	goat #7075	Cell Signaling	1:1000
GAPDH	(14C10) rabbit mAb #2118	Cell Signaling	1:1000
ERO1α	rabbit polyclonal #3264	Cell Signaling	1:1000
XBP1	(D2C1F) rabbit mAb #12782	Cell Signaling	1:1000
Phospho-eIF2α	(L57A5) mouse mAb #2103	Cell Signaling	1:1000
BiP	(C50B12) rabbit mAb #3177	Cell Signaling	1:1000

Supplementary Table S10 – shRNA used for PDI and TXN knock-down

Catalog no.	Target	shRNA sequence
SHC002V	Non-Mammalian shRNA Control	Not known
TRCN0000049193	PDI (a)	CCGGCGAGTTCTTTGGCCTGAAGAACTCG AGTTCTTCAGGCCAAAGAACTCGTTTTTG
TRCN0000049194	PDI (b)	CCGGGTGTGGTCACTGCAAACAGTTCTCG AGAACTGTTTGCAGTGACCACACTTTTTG
TRCN0000290651	PDI (c)	CCGGGTGTGGTCACTGCAAACAGTTCTCG AGAACTGTTTGCAGTGACCACACTTTTTG
TRCN0000049196	PDI (d)	CCGGCGACAGGACGGTCATTGATTACTCG AGTAATCAATGACCGTCCTGTCGTTTTTG
TRCN0000296736	PDI (e)	CCGGTGCTGTTCTTGCCCAAGAGTGCTCG AGCACTCTTGGGCAAGAACAGCATTTTTG
TRCN0000064279	TXN (a)	CCGGGCTTCAGAGTGTGAAGTCAAACTCG AGTTTGACTTCACACTCTGAAGCTTTTTG
TRCN0000064278	TXN (b)	CCGGGCAGGTGATAAACTTGTAGTACTCG AGTACTACAAGTTTATCACCTGCTTTTTG
TRCN0000064280	TXN (c)	CCGGGATGTGGATGACTGTCAGGATCTCG AGATCCTGACAGTCATCCACATCTTTTTG
TRCN0000369941	TXN (d)	CCGGATCAAGCCTTTCTTTCATTCCCTCGA GGGAATGAAAGAAAGGCTTGATTTTTTG
TRCN0000007305	CEBPA (a)	CCGGGCTGGAGCTGACCAGTGACAACTCG AGTTGTCACTGGTCAGCTCCAGCTTTTT
TRCN0000007307	CEBPA (b)	CCGGCAAGAAGTCGGTGGACAAGAACTCG AGTTCTTGTCCACCGACTTCTTGTTTTT
TRCN0000356198	CEBPA (c)	CCGGCCCGGCAACTCTAGTATTTAGCTCG AGCTAAATACTAGAGTTGCCGGGTTTTTG

Supplementary Table S11 – AML patients data

No	Diagnosis	Age at diagnosis	Sex	FAB	Molecular signature	Karyotype	Blasts in bone marrow	WBC [$\times 10^3$/ µl]	RBC [$\times 10^6$/ µl]	Hgb [g/ dl]	PLT [$\times 10^3$/ µl]	Neut [$\times 10^3$/ µl]
Pt 1	AML/ MDS	36	F			chr. 7 monosomy	40	19.45	2.8	8.7	50	45.5
Pt 2	AML	43	F	AML-M5	NPM1 mutation	normal karyotype		39.54	4.15	12.6	143	--
Pt 3	AML	59	M		NPM1 mutation	chr. 8 trisomy		41.07	4.69	11.5	26	--
Pt 4	AML	27	M	AML-M4				66.02	4.28	10.4	34	9.11
Pt 5	mixed karyotype AML	25	F					14.7	2.92	5	22	--
Pt 6	atypical AML (CML->AML-M4)	58	M	AML-M4			28					

Abbreviations used: AML – acute myeloid leukemia; chr – chromosome; CML – chronic myeloid leukemia; F – female; FAB – French-American-British AML classification; Hgb – hemoglobin; M – male; MDS – myelodysplastic syndrome; Neut – neutrophils; PLT – platelets; RBC – red blood cells; WBC – white blood cells.

Descriptions to supplementary figures and a video file

Supplementary Fig. S1. SK053 exerts anti-leukemic effects and induces differentiation of AML cell lines *in vitro*. **A,** MOLM14, NB4, and KG1 cells were incubated with serial dilutions of SK053 for up to 5 days. Each day the number of dead cells was evaluated with trypan blue exclusion. Graphs present mean percentage of dead cells comparing to controls ±SD; *P<0.05 vs controls, one-way ANOVA with Dunnett's post-hoc test, n=6. **B,** MOLM14, NB4, and KG1 cells were incubated with serial dilutions of SK053 for up to 5 days. Each day the number of living cells was evaluated with trypan blue exclusion. Graphs present mean cell number ±SD; *P<0.05 vs controls, one-way ANOVA with Dunnett's post-hoc test, n=6. **C,** Semi-quantitative colorimetric NBT reduction assay in MOLM14, NB4, and KG1 cells incubated for 5 days with indicated SK053 concentrations; graphs present mean % increase vs control ±SD; *P<0.05 vs controls, one-way ANOVA with Dunnett's post-hoc test, n=3.

Supplementary Fig. S2. Diagram of RNA sequencing data analysis pipeline used for differential gene expression (DGE) analysis in the SK053-treated HL-60 cells.

Supplementary Fig. S3. Differential gene expression (DGE) analysis of HL-60 cells treated for 48 h with 10 μM SK053 vs DMSO treated controls. **A,** Volcano plot of genes differentially expressed between the cells treated for 48 h with SK053 and control cells (DMSO). **B,** Diagram of significantly enriched Biological Process GO nodes corresponding to the results of DGE results obtained for cells treated for 48 h with 10 μM SK053. The yellow and orange nodes represent terms with significant enrichment, with different color shades representing various degrees of significance i.e. from 1.00E-2 (yellow) up to <1.00E-6 (red). **C,** Diagram of significantly enriched Molecular Function GO nodes corresponding to the results of DGE results obtained for cells treated for 48 h with 10 μM SK053. The yellow and orange nodes represent terms with significant enrichment, with different color shades representing various degrees of significance i.e. from 1.00E-2 (yellow) up to <1.00E-3 (red).

Supplementary Fig. S4. Differential gene expression (DGE) analysis of HL-60 cells treated for 120 h with 10 μM SK053 vs DMSO treated controls. **A,** Volcano plot of genes differentially expressed between the cells treated for 120 h with 10 μM SK053 and control cells (DMSO). **B,** Diagram of significantly enriched Biological Process GO nodes corresponding to the results of DGE results obtained for cells treated for 120 h with 10 μM SK053. The yellow and orange nodes represent terms with significant enrichment, with different color shades representing various degrees of significance i.e. from 1.00E-2 (light yellow) up to <1.00E-7 (orange). **C,** Diagram of significantly enriched Molecular Function GO nodes corresponding to the results of DGE results obtained for cells treated for 120 h with 10 μM SK053. The yellow and orange nodes represent terms with significant enrichment, with different color shades representing various degrees of significance i.e. from 1.00E-2 (light yellow) up to <1.00E-7 (orange).

Supplementary Fig. S5. SK053 induces ER stress in HL-60 cells. Representative Western blot results showing UPR and ER stress markers induction in HL-60 cells upon incubation with 10 μM SK053, GAPDH levels served as a loading control.

Supplementary Fig. S6. Evaluation of cell growth and differentiation in HL-60 and MOLM14 cells upon TXN knock-down. **A**, Control HL-60 cells and HL-60 cells transduced with non-targeting (NTC) or TXN [TXN(a)]-targeting shRNA lentiviral particles were counted daily in trypan blue from day [d] 1 till day 10. **B**, Western blot showing the efficacy of TXN knock-down in HL-60 and MOLM14 cell lines transduced with TXN-targeting shRNA [(TXN(b) or TXN(c)]-encoding lentiviruses. GAPDH served as a loading control. **C**, Growth of HL-60 cells transduced with non-targeting (NTC) or TXN-targeting [(TXN(b) or TXN(c)] shRNA. Cells were counted daily in trypan blue from day 1 till day 9. *$p<0.05$ vs NTC in two-tailed Student's *t* test. **D**, Growth of MOLM14 cells transduced with non-targeting (NTC) or TXN-targeting [(TXN(b) or TXN(c)] shRNA. Cells were counted daily in trypan blue from day 1 till day 9. *$p<0.05$ vs NTC in two-tailed Student's *t* test. **E**, Mean percentage ±SD of AML cells modified with non-targeting (NTC) or TXN-targeting [(TXN(b) or TXN(c)] shRNA, expressing CD11b myeloid marker determined in flow cytometry, N=4, p values (p) calculated vs NTC, two-tailed Student's *t* test, NS-not significant.

Supplementary Fig. S7. Evaluation of cell growth and differentiation in HL-60 and cells upon CEBPA knock-down **A**, Western blot showing C/EBPα levels in two distinct sets (1 and 2) of HL-60 cells transduced with non-targeting (NTC) or PDI-targeting [PDI(d)] shRNA. GAPDH served as a loading control. **B**, Western blot showing the efficacy of CEBPA knock-down in HL-60 cells transduced with CEBPA-targeting shRNA [CEBPA(a) or CEBPA(c)]-encoding lentiviruses. GAPDH served as a loading control. **C**, Growth of HL-60 cells modified with CEBPA [CEBPA(a) or CEBPA(c)]-targeting shRNA and incubated with 5 or 10 μM SK053. Cells were counted daily in trypan blue from day 1 till day 8. **D**, Mean percentage ±SD of HL-60 cells modified with non-targeting (NTC) or CEBPA [CEBPA(a) or CEBPA(c)]-targeting shRNA, expressing CD11b myeloid marker determined in flow cytometry, N=2.

Supplementary Fig. S8. Chemical structures of compounds. **A,** Chemical structure of SK053. **B,** Chemical structure of SK-BIO – a biotinylated SK053 analog. **C,** Chemical structure of SK-IN – an inactive, biotinylated SK053 analogue that lacks the electrophilic double bond. **D,** Chemical structure of SK053 showing the localization of the leaving group and truncated form of the compound. **E,** Potential mechanism of SK053 binding to catalytic cysteines in PDI, 1 or 2 truncated SK053 molecules bind to PDI catalytic site.

Supplementary Fig. S9. Proteomic assessment of SK053 binding site in the human PDI (huPDI). **A,** Amino acid sequence of huPDI showing peptides identified by mass spectrometry (bold red). The peptide containing Cys residue with SK053 modification is underlined. (**b-d**) Example MS/MS data for the peptide 400KNVFVEFYAPWCGHCK415 from huPDI. MS/MS fragmentation was performed on a Thermo Orbitrap Velos coupled with Waters nanoAcquity UPLC and data were analyzed by Mascot software. This peptide had a

Mascot ion score of 56, precursor mass of 2209.054, charge state of +3. **B,** The MS/MS fragmentation spectrum with y-series and b-series ions labeled. **C,** Table of detected masses as annotated by Mascot. Bold italic red indicates that the ion series contributed to the peptide score. Bold red indicates the number of matches in the ion series is greater than would be expected by chance alone, suggesting that the ion series is present in the spectrum. Non-bold red means that the number of matches in the ion series is no greater than would be expected by chance. Masses indicated in black type were not detected in the spectrum. C* indicates the most probable site of SK053 modification on Cys414. **D,** Alternate Mascot site analysis indicates another putative SK053 binding site on residue Cys411 (marked as C#). **E,** SK053 binds to the 4th thioredoxin-like domain of huPDI (PDIA1-d4): the recombinant PDIA1-d4 protein was incubated without (left) and with SK053 in a molar ratio 1:10 (right). The mass shift observed in the right panel corresponds to two molecules of the inhibitor after the elimination of the leaving group (2 × 282 Da), according to the mechanism described previously.[3]

Supplementary Fig. S10. Covalent docking of SK053 to two cavities in the 4th thioredoxin-like domain in human PDI. **A,** Truncated SK053 molecule (molecule without the leaving group, Supplementary Fig. S6d) bound to Cys397 of huPDI. The polar contacts between the ligand and the protein are shown with a dotted, yellow line. The ligand is placed in the "primary" cavity. **B,** Truncated SK053 molecule bound to Cys400 of huPDI. The polar contacts between the ligand and the protein are shown with a dotted, yellow line. The ligand is placed in the "secondary" cavity. **C,** Two truncated SK053 molecules bound to either Cys400 or Cys397of huPDI. The ligand can be either placed in the "primary" cavity or the "secondary" cavity.

Supplementary Video S1. Two putative binding sites of hPDI are located on the opposite site of the helix harboring active site cysteines. Molecular docking with GOLD suggests that both 'primary' binding site (depict cyan on the protein surface) and 'secondary' binding site (magenta) are equally probable to host SK053 molecule. Full atom representations of both binding sites are presented in Supplementary Fig. S10.

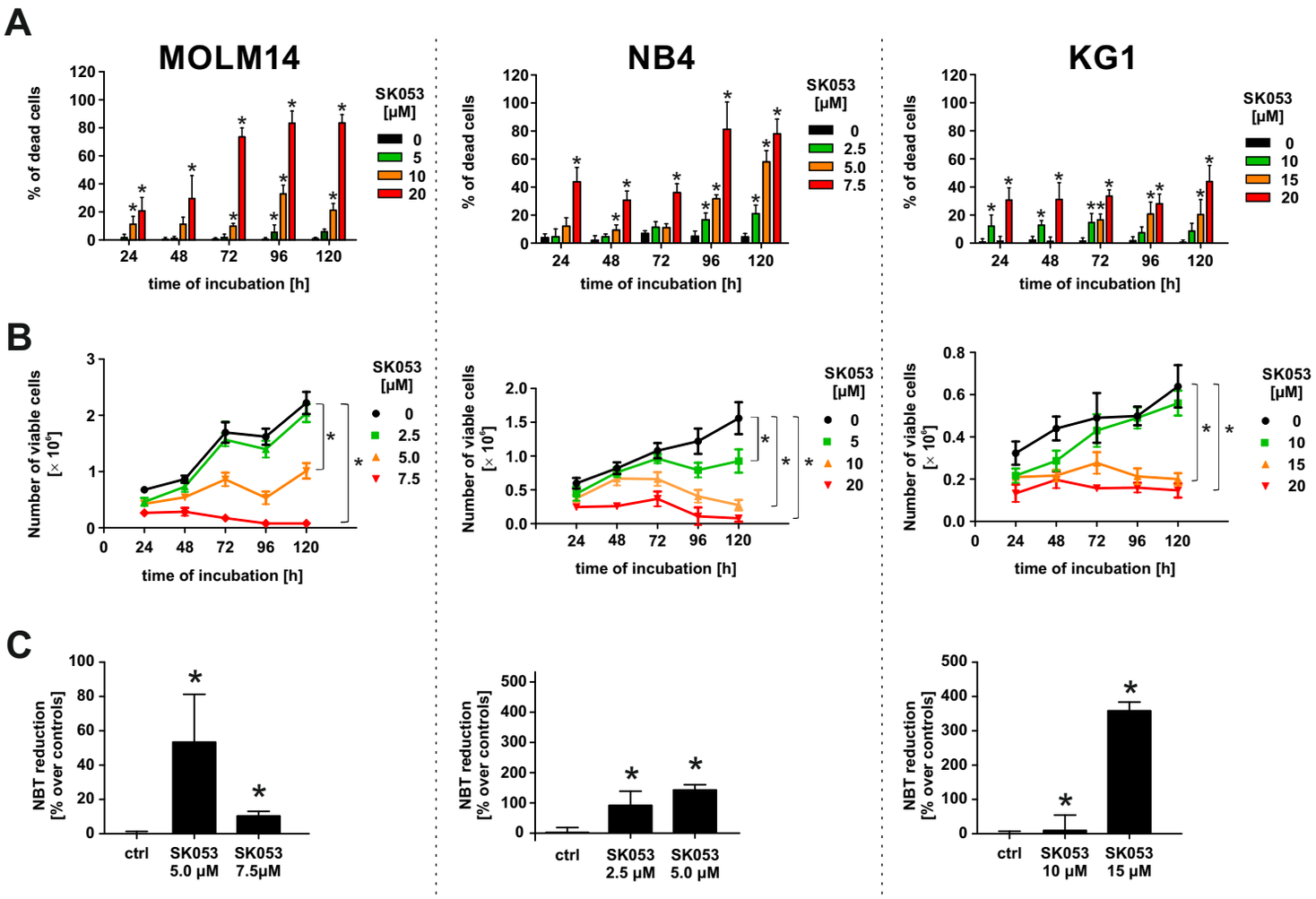

Supplementary Figure S1

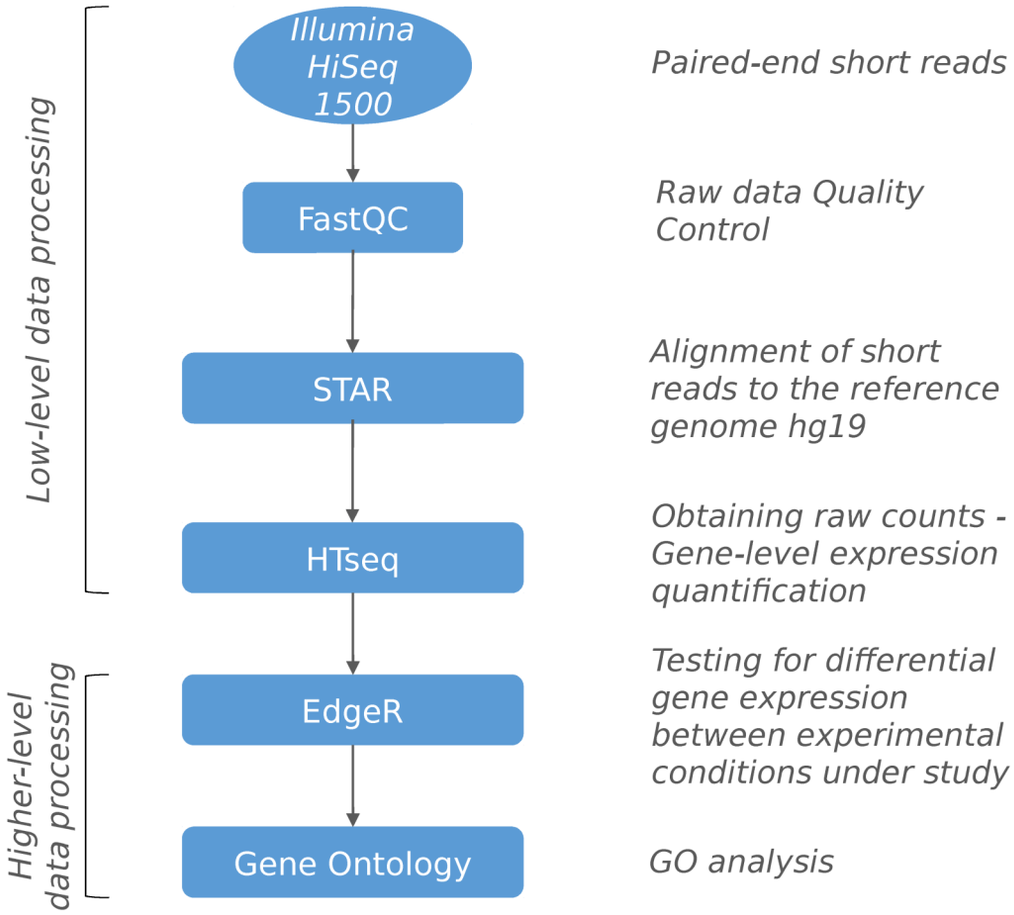

Supplementary Figure S2

A

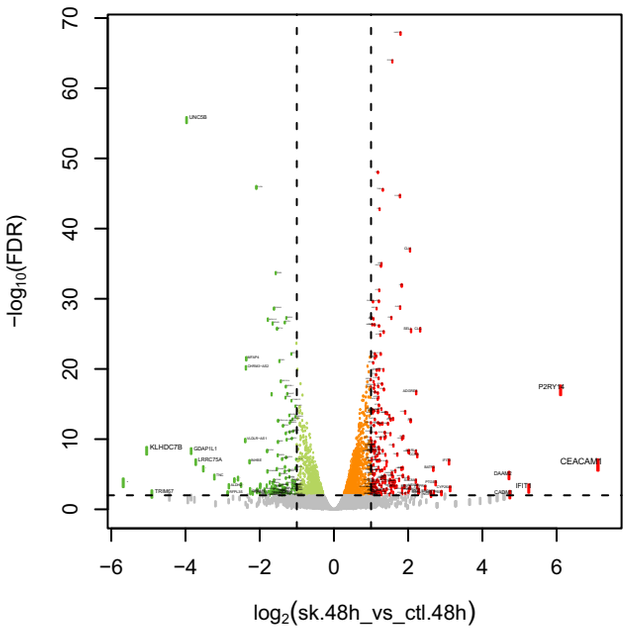

B

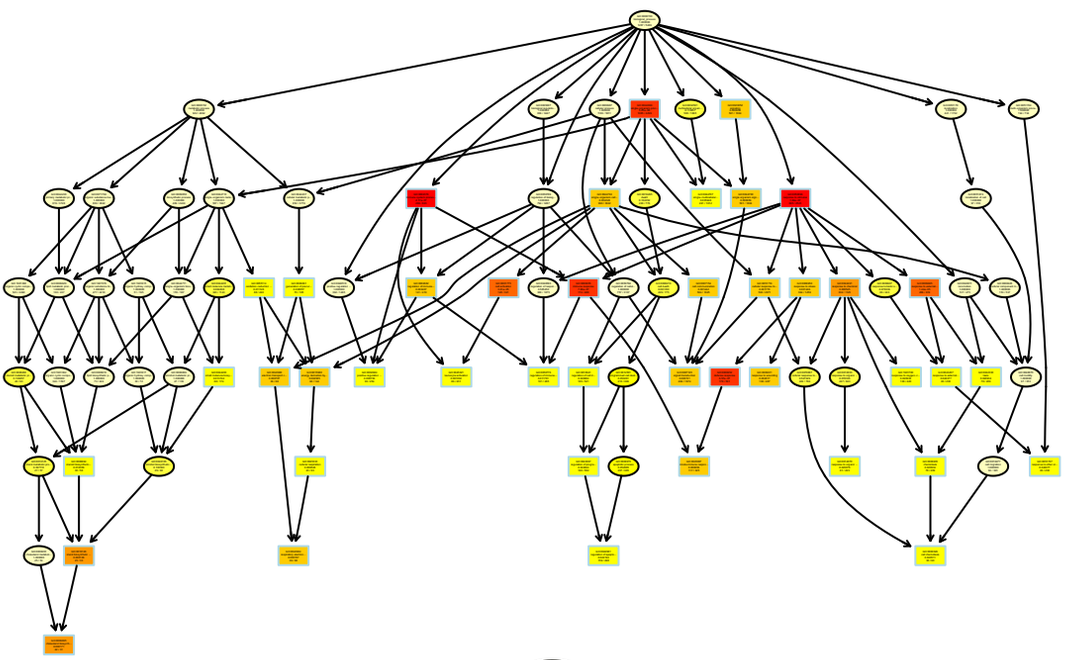

C

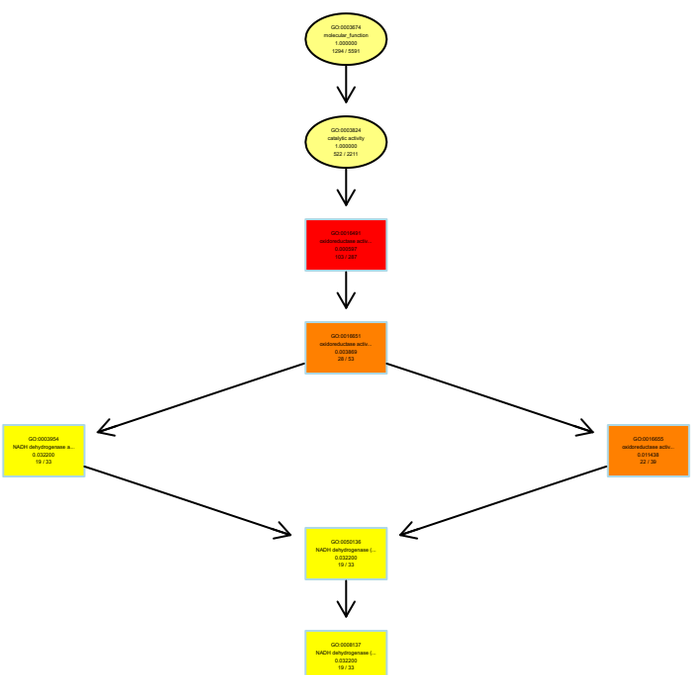

Supplementary Figure S3

A

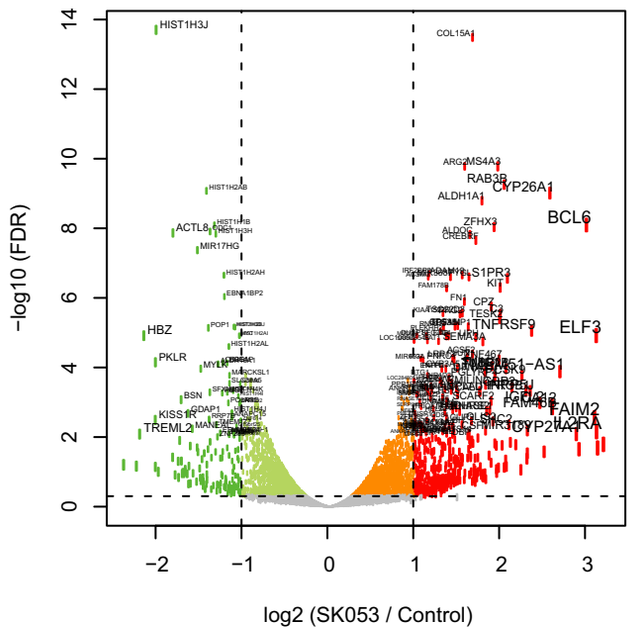

B

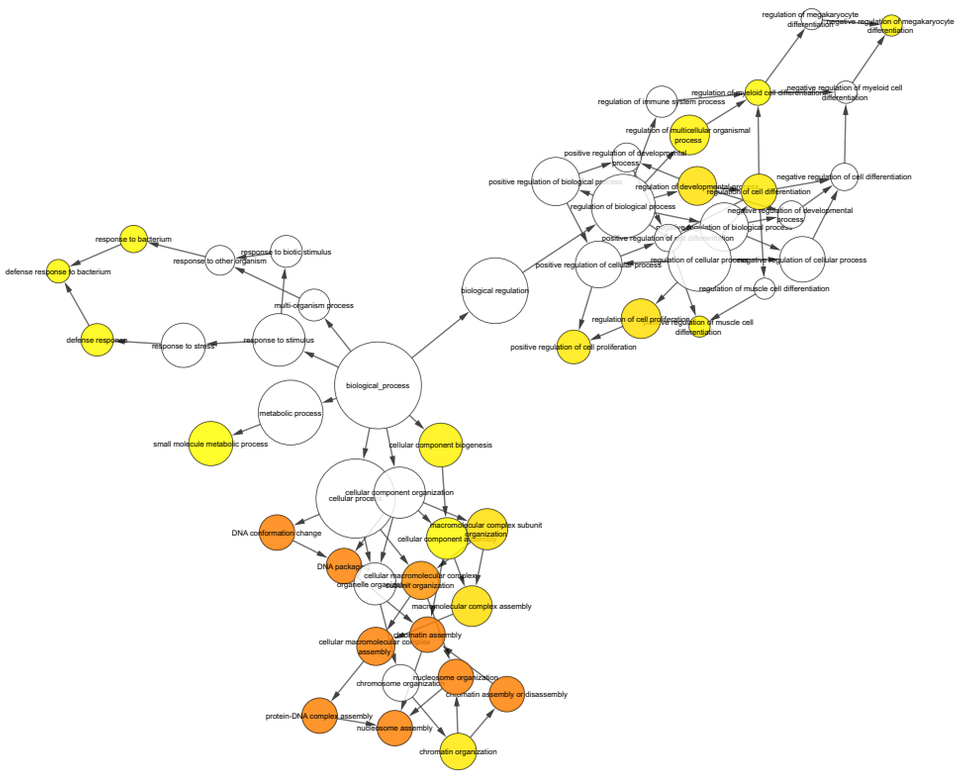

C

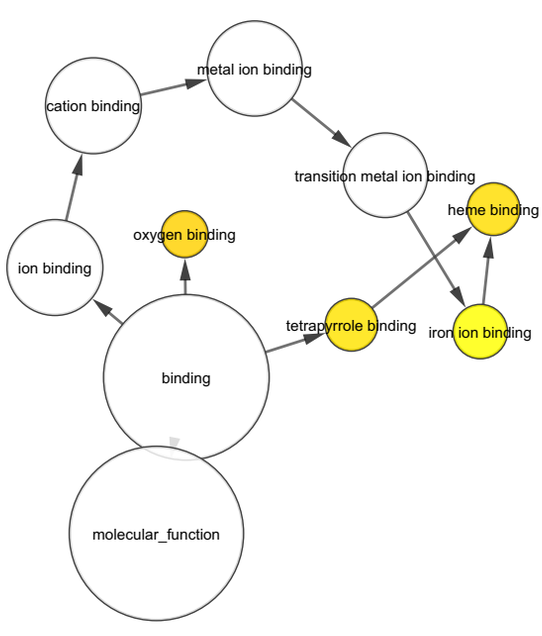

Supplementary Figure S4

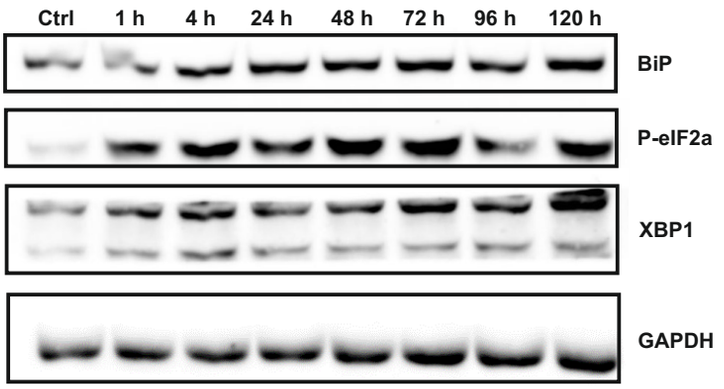

Supplementary Figure S5

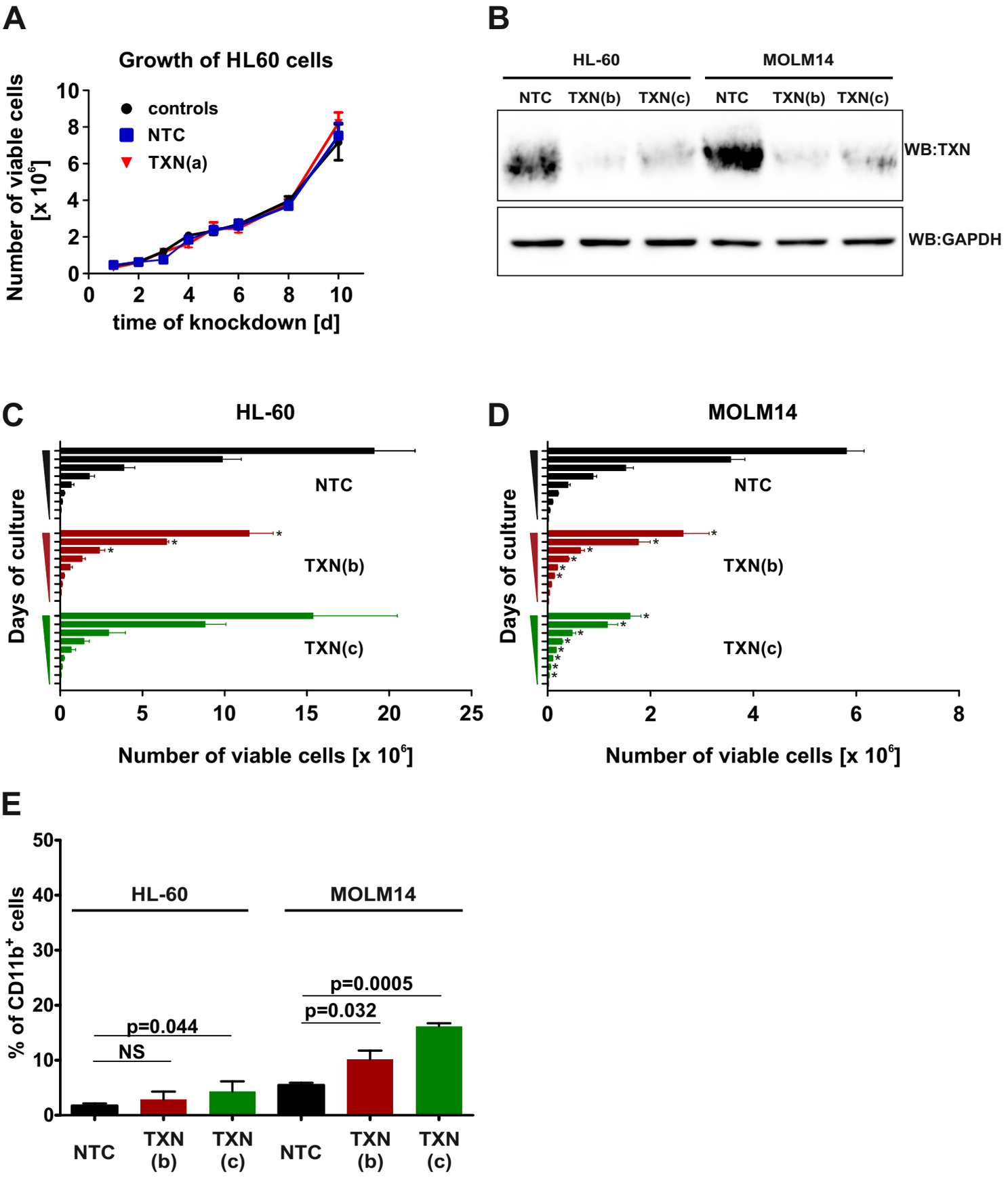

Supplementary Figure S6

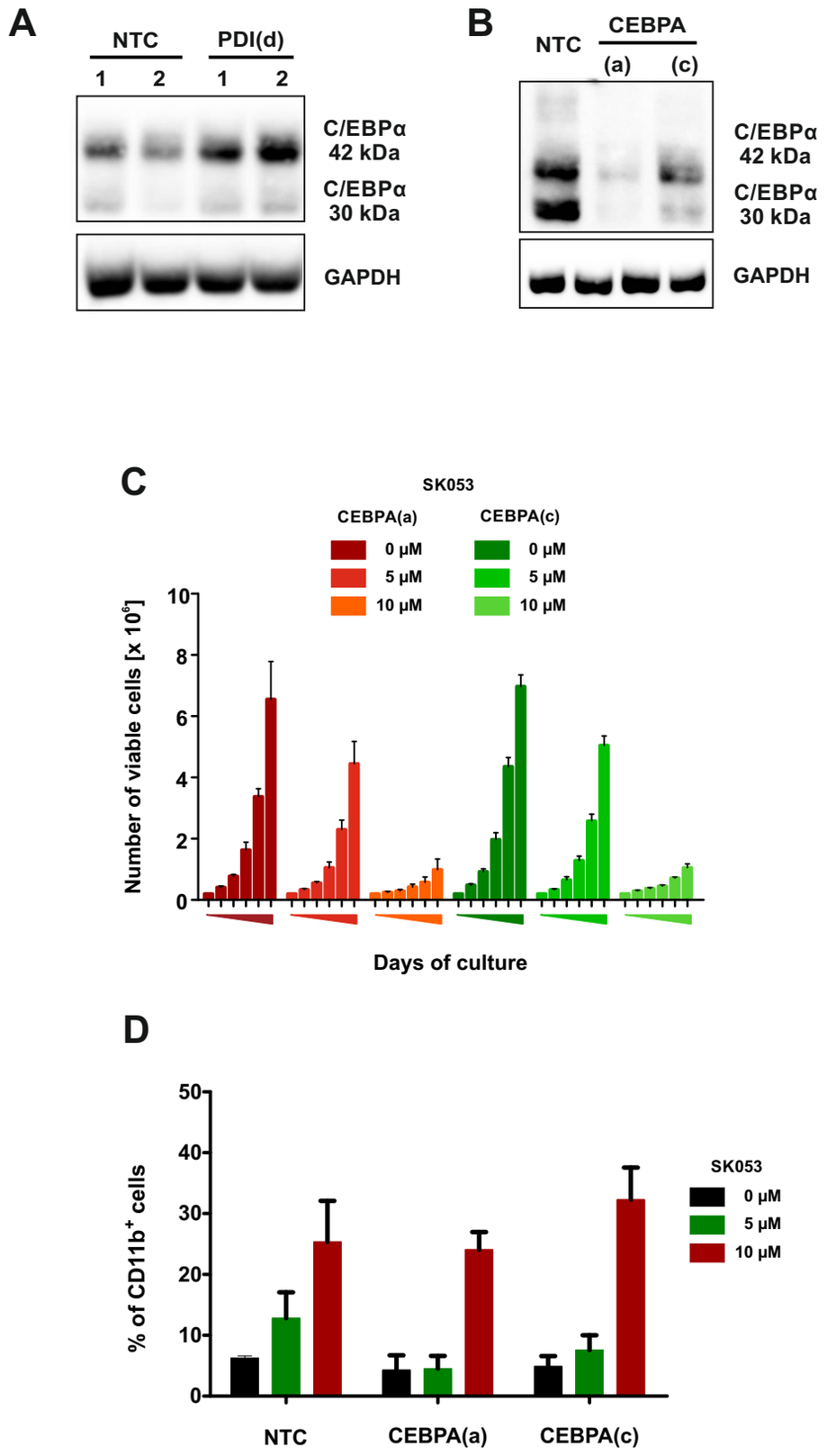

Supplementary Figure S7

A

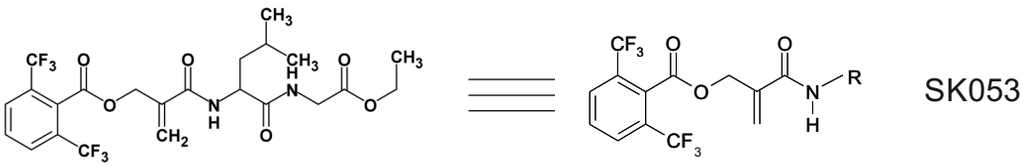

SK053

B

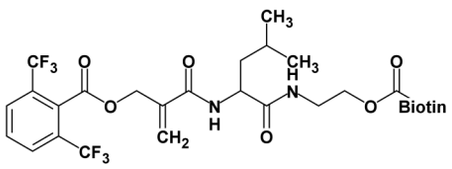

SK053-biotin = SK-BIO

C

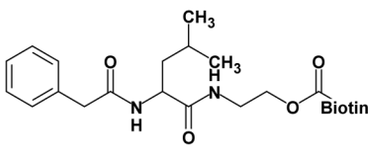

inactive biotinylated SK053 analog = SK-IN

D

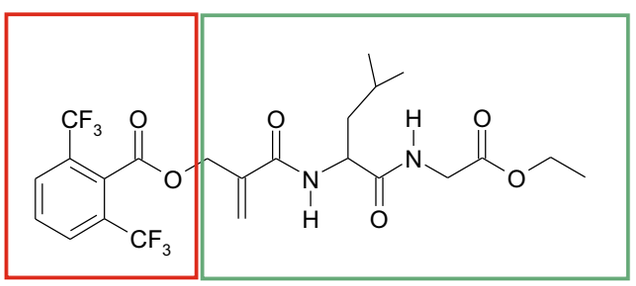

leaving group truncated SK053

E

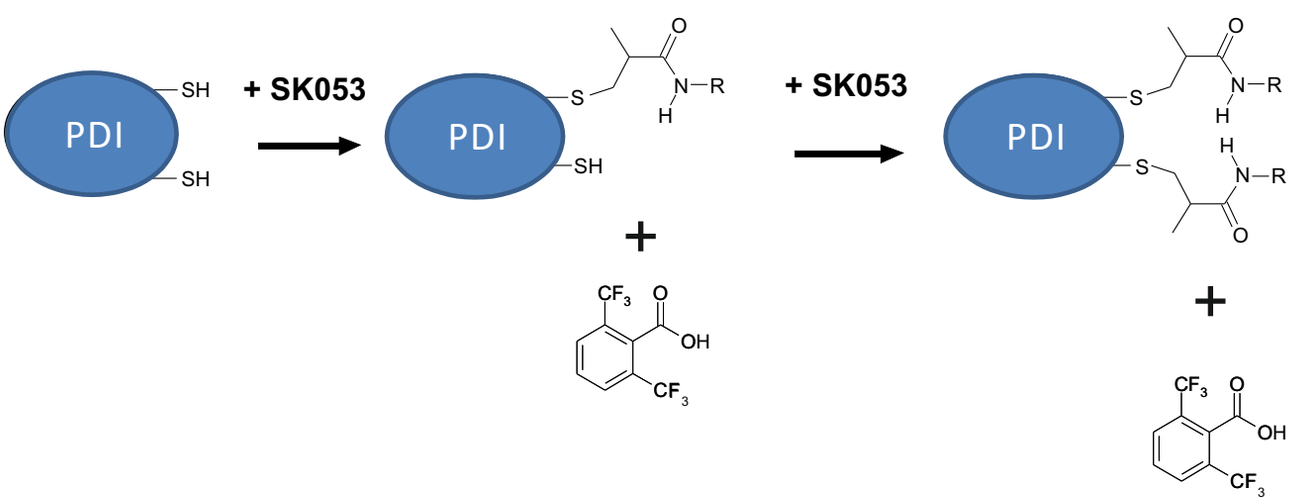

Supplementary Figure S8

A

```
  1 MKHHHHHHPM SDYDIPTTEN LYFQGAMASV PDAPEEEDHV LVLRKSNFAE
 51 ALAAHKYLLV EFYAPWCGHC KALAPEYAKA AGKLKAEGSE IRLAKVDATE
101 ESDLAQQYGV RGYPTIKFFR NGDTASPKEY TAGREADDIV NWLKKRTGPA
151 ATTLPDGAAA ESLVESSEVA VIGFFKDVES DSAKQFLQAA EAIDDIPFGI
201 TSNSDVFSKY QLDKDGVVLF KKFDEGRNNF EGEVTKENLL DFIKHNQLPL
251 VIEFTEQTAP KIFGGEIKTH ILLFLPKSVS DYDGKLSNFK TAAESFKGKI
301 LFIFIDSDHT DNQRILEFFG LKKEECPAVR LITLEEEMTK YKPESEELTA
351 ERITEFCHRF LEGKIKPHLM SQELPEDWDK QPVKVLVGKN FEDVAFDEKK
401 NVFVEFYAPW CGHCKQLAPI WDKLGETYKD HENIVIAKMD STANEVEAVK
451 VHSFPTLKFF PASADRTVID YNGERTLDGF KKFLESGGQD GAGDDDDLED
501 LEEAEEPDME EDDDQKAVKD EL
```

B

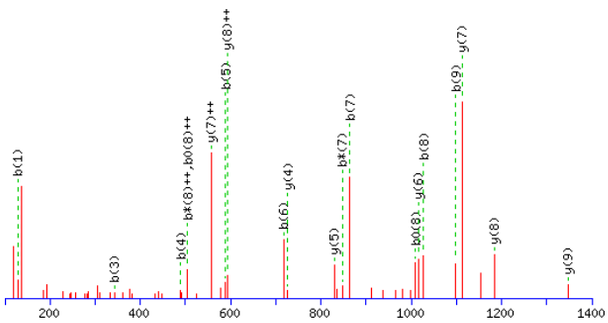

C

#	b	b^{++}	b*	b^{*++}	b^{0}	b^{0++}	Seq.	y	y^{++}	y*	y^{*++}	y^{0}	y^{0++}	#
1	*129.1022*	65.0548	112.0757	56.5415			K							16
2	243.1452	122.0762	226.1186	113.5629			N	2081.9612	1041.4842	2064.9347	1032.9710	2063.9506	1032.4790	15
3	*342.2136*	171.6104	325.1870	163.0972			V	1967.9183	984.4628	1950.8917	975.9495	1949.9077	975.4575	14
4	*489.2820*	245.1446	472.2554	236.6314			F	1868.8499	934.9286	1851.8233	926.4153	1850.8393	925.9233	13
5	*588.3504*	294.6788	571.3239	286.1656			V	1721.7814	861.3944	1704.7549	852.8811	1703.7709	852.3891	12
6	*717.3930*	359.2001	700.3665	350.6869	699.3824	350.1949	E	1622.7130	811.8602	1605.6865	803.3469	1604.7025	802.8549	11
7	*864.4614*	432.7343	847.4349	424.2211	846.4508	423.7291	F	1493.6704	747.3389	1476.6439	738.8256			10
8	*1027.5247*	514.2660	1010.4982	505.7527	1009.5142	505.2607	Y	*1346.6020*	673.8047	1329.5755	665.2914			9
9	*1098.5619*	549.7846	1081.5353	541.2713	1080.5513	540.7793	A	*1183.5387*	592.2730	1166.5121	583.7597			8
10	1195.6146	598.3109	1178.5881	589.7977	1177.6041	589.3057	P	*1112.5016*	556.7544	1095.4750	548.2412			7
11	1381.6939	691.3506	1364.6674	682.8373	1363.6834	682.3453	W	*1015.4488*	508.2280	998.4223	499.7148			6
12	1484.7031	742.8552	1467.6766	734.3419	1466.6926	733.8499	$C^{\#}$	*829.3695*	415.1884	812.3430	406.6751			5
13	1541.7246	771.3659	1524.6980	762.8527	1523.7140	762.3606	G	*726.3603*	363.6838	709.3338	355.1705			4
14	1678.7835	839.8954	1661.7569	831.3821	1660.7729	830.8901	H	669.3389	335.1731	652.3123	326.6598			3
15	2063.9506	1032.4790	2046.9241	1023.9657	2045.9401	1023.4737	C^{*}	532.2799	266.6436	515.2534	258.1303			2
16							K	147.1128	74.0600	130.0863	65.5468			1

D

Score	Mr(calc)	Delta	Sequence	Site Analysis
56.0	2209.0489	0.0059	KNVFVEFYAPWCGHCK	SK053 $C15^{*}$ 87.57%
47.5	2209.0489	0.0059	KNVFVEFYAPWCGHCK	SK053 $C12^{\#}$ 12.43%

E

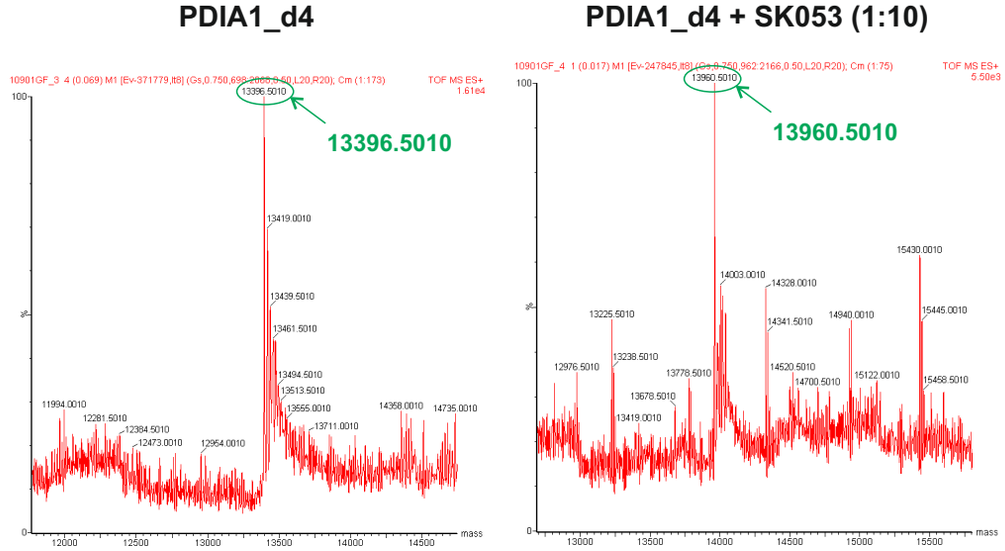

Supplementary Figure S9

A

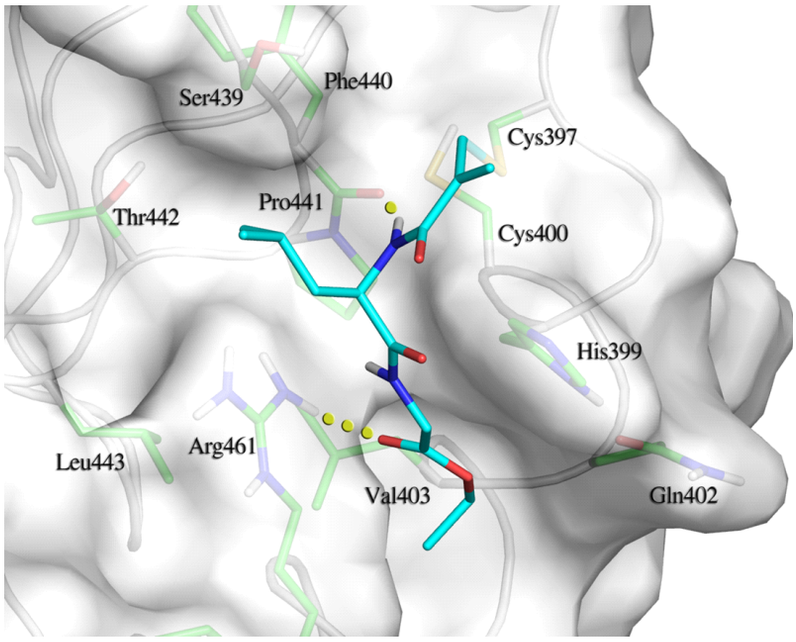

B

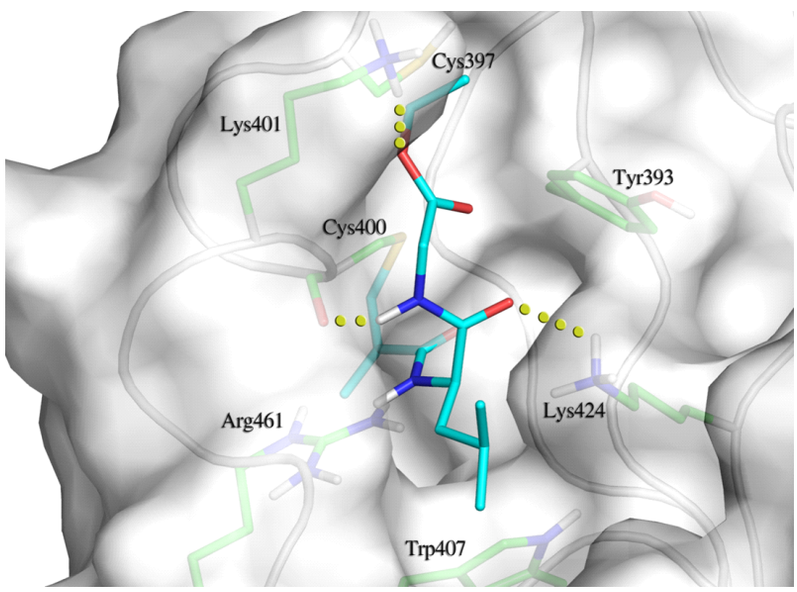

C

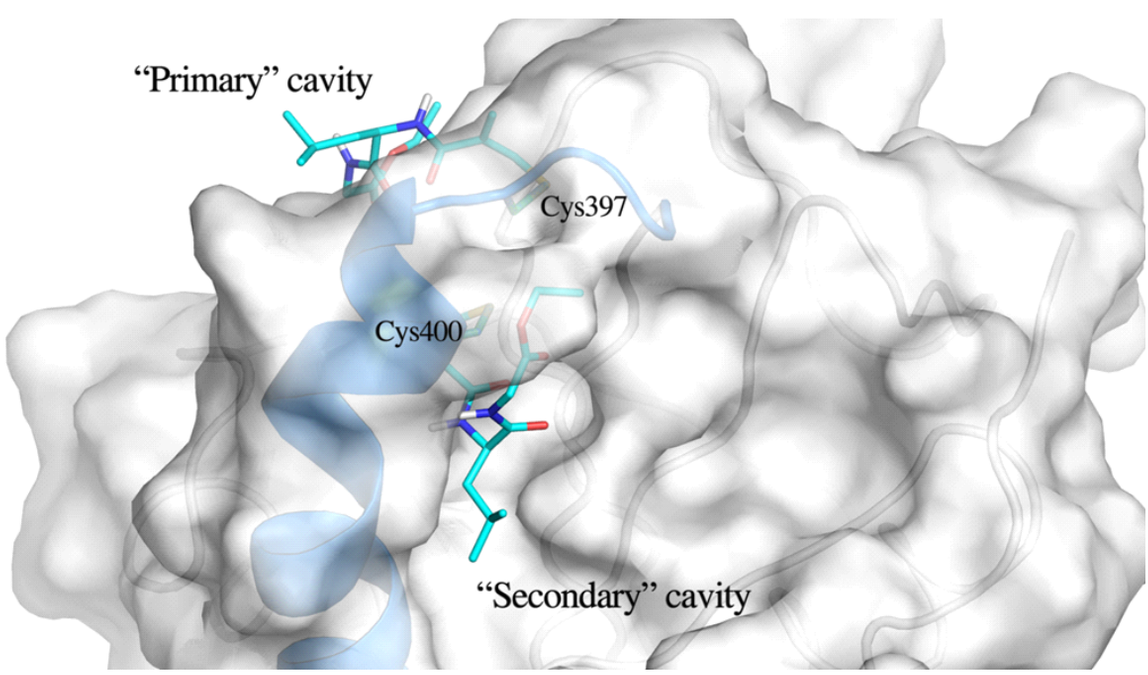

Supplementary Figure S10